

Rare charm decays at LHCb

Christopher Thomas*[†]

University of Oxford

E-mail: c.thomas2@physics.ox.ac.uk

We present two searches for rare charm decays by the LHCb collaboration using data corresponding to an integrated luminosity of 1 fb^{-1} recorded in 2011. The first is a search for $D^0 \rightarrow \mu^+ \mu^-$ decays for which the upper limit on the branching fraction at the 95% C.L. is found to be

$$\mathcal{B}(D^0 \rightarrow \mu^+ \mu^-) < 1.3 \times 10^{-8}.$$

The second search presented is for $D_{(s)}^\pm \rightarrow \pi^\pm \mu^+ \mu^-$ and $D_{(s)}^\pm \rightarrow \pi^\mp \mu^\pm \mu^\pm$ decays. Upper limits on the branching fractions at the 95% C.L. are determined to be

$$\mathcal{B}(D^\pm \rightarrow \pi^\pm \mu^+ \mu^-) < 8.3 \times 10^{-8},$$

$$\mathcal{B}(D_s^\pm \rightarrow \pi^\pm \mu^+ \mu^-) < 4.8 \times 10^{-7},$$

$$\mathcal{B}(D^\pm \rightarrow \pi^\mp \mu^\pm \mu^\pm) < 2.5 \times 10^{-8},$$

$$\mathcal{B}(D_s^\pm \rightarrow \pi^\mp \mu^\pm \mu^\pm) < 1.4 \times 10^{-7}.$$

14th International Conference on B-Physics at Hadron Machines

April 8-12, 2013

Bologna, Italy

*Speaker.

[†]On behalf of the LHCb collaboration.

1. Introduction

Flavour-changing neutral currents (FCNCs) are highly suppressed in the Standard Model (SM). This is particularly true in the charm sector for which Glashow-Iliopoulos-Maiani (GIM) suppression plays a significant role. Decays that proceed solely via FCNCs, with no tree diagram, are conventionally denoted ‘rare’. Physical processes that exist beyond the SM (BSM) can potentially enhance the branching fractions of rare decays; one example is R -parity violating supersymmetry [1, 2]. Precision measurements of rare charm decays could therefore reveal the presence of any BSM physics.

In these proceedings we present two searches for rare charm decays by the LHCb collaboration. The first is for D^0 decays to the final state $\mu^+\mu^-$ [3] and the second is for $D_{(s)}^\pm$ decays to $\pi^\pm\mu^+\mu^-$ and $\pi^\mp\mu^\pm\mu^\pm$ [4], described in Sections 2 and 3, respectively. The two final states share similar topologies and the analyses therefore have several features in common. Both analyses use data recorded by LHCb in 2011 at a centre-of-mass energy of 7 TeV.

2. $D^0 \rightarrow \mu\mu$

The decay $D^0 \rightarrow \mu\mu$ is very rare in the SM; in addition to GIM suppression the decay is helicity suppressed. Long-distance contributions, particularly the $\gamma\gamma$ intermediate state, are anticipated to dominate. The SM predicts a branching fraction $\mathcal{B}(D^0 \rightarrow \mu^+\mu^-) < 6 \times 10^{-11}$ at the 90% confidence level (C.L.).

The search for $D^0 \rightarrow \mu^+\mu^-$ is performed on a data sample collected by LHCb corresponding to an integrated luminosity of 0.9 fb^{-1} . Decays of $D \rightarrow \mu^+\mu^-$ (where D indicates D^0 or \bar{D}^0) are reconstructed in the decay chain $D^{*\pm} \rightarrow D(\mu^+\mu^-)\pi^\pm$, where the D^* is produced at the pp interaction vertex and the charge of the pion tags the flavour of the D . The analysis exploits the kinematically similar decay channel $D^{*\pm} \rightarrow D(\pi^+\pi^-)\pi^\pm$ to normalise the yield of signal decays. Two further decays, $J/\psi \rightarrow \mu^+\mu^-$ and $D^{*\pm} \rightarrow D(K^\pm\pi^\mp)\pi^\pm$, are used as control channels. A multivariate selection is used to reduce the level of combinatorial background and particle identification criteria are used to reduce backgrounds in which a π or K is misidentified as a muon.

The branching fraction $\mathcal{B}(D^0 \rightarrow \mu^+\mu^-)$ is determined according to the formula

$$\mathcal{B}(D^0 \rightarrow \mu^+\mu^-) = \frac{N(\mu^+\mu^-)}{N(\pi^+\pi^-)} \times \frac{\varepsilon(\pi^+\pi^-)}{\varepsilon(\mu^+\mu^-)} \times \mathcal{B}(D^0 \rightarrow \pi^+\pi^-) = \alpha \times N(\mu^+\mu^-), \quad (2.1)$$

where $N(X)$ and $\varepsilon(X)$ are the yield and selection efficiency of the final state X , respectively. Trigger and reconstruction efficiencies are determined from Monte Carlo simulated data and corrected using data-driven methods. The value of $\mathcal{B}(D^0 \rightarrow \pi^+\pi^-)$ is taken from Ref. [5].

The yields of $D^0 \rightarrow \mu^+\mu^-$ and $D^0 \rightarrow \pi^+\pi^-$ candidates are determined from two-dimensional unbinned maximum likelihood fits to the reconstructed D mass, m_{D^0} , and the difference between the D^* and D masses, Δm . The fits to $D \rightarrow \pi^+\pi^-$ candidates are illustrated in Fig. 1 and those to $D \rightarrow \mu^+\mu^-$ candidates are shown in Fig. 2. The parameter α is calculated to be $(1.96 \pm 0.23) \times 10^{-10}$.

In Fig. 2, no significant excess over the background is observed. The CL_s method [6, 7] is used to determine the upper limit on the $D^0 \rightarrow \mu^+\mu^-$ branching fraction

$$\mathcal{B}(D^0 \rightarrow \mu^+\mu^-) < 1.3 \times 10^{-8} \quad (95\% \text{ C.L.}). \quad (2.2)$$

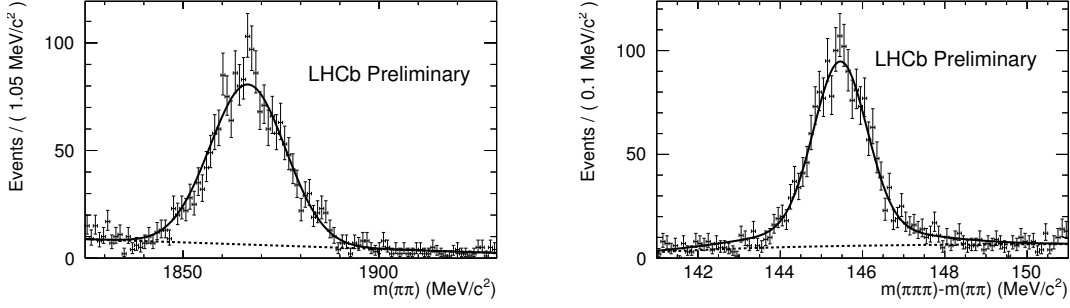


Figure 1: Fits to (left) m_{D^0} , (right) Δm for the normalisation channel $D^0 \rightarrow \pi^+\pi^-$. The total PDF is the solid black line and the combinatorial background is the dotted black line.

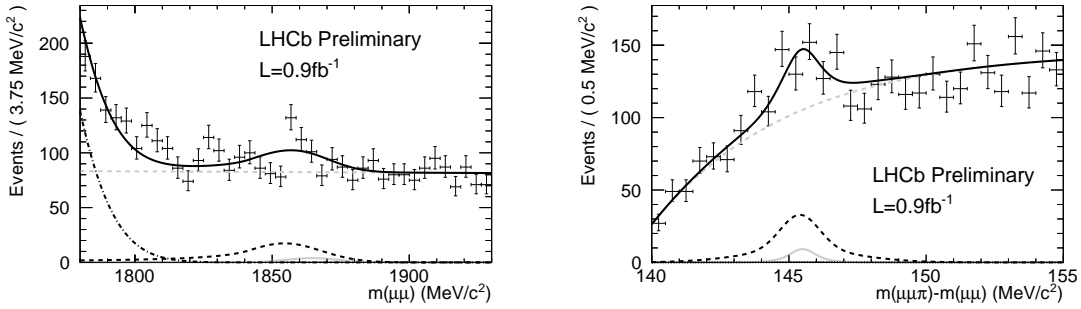


Figure 2: Fits to (left) m_{D^0} , (right) Δm for $D^0 \rightarrow \mu^+\mu^-$. The signal (barely visible) is the solid grey line, the $D^0 \rightarrow \pi^+\pi^-$ peaking background is the black dashed line, the $D^0 \rightarrow K^+\pi^-$ background is the black dotted line and the combinatorial background is the grey dashed line.

The previous best upper limit was 1.4×10^{-7} [8]; the SM prediction is several orders of magnitude lower still.

3. $D_{(s)}^\pm \rightarrow \pi^\pm \mu^+ \mu^-$ and $D_{(s)}^\pm \rightarrow \pi^\mp \mu^\pm \mu^\pm$

Decays of both D^\pm and D_s^\pm mesons to the final states $\pi^\pm \mu^+ \mu^-$ and $\pi^\mp \mu^\pm \mu^\pm$ are of interest to this analysis. The branching fraction of the decay $D^\pm \rightarrow \pi^\pm \mu^+ \mu^-$ is predicted to be in the range $1\text{--}3 \times 10^{-9}$ [9, 10, 11]. The equivalent D_s decay occurs via weak annihilation (WA) and is useful as a normalisation channel; it is essential to distinguish WA from FCNC contributions in $D^\pm \rightarrow \pi^\pm \mu^+ \mu^-$ decays.

Lepton number violating processes such as $D_{(s)}^\pm \rightarrow \pi^\mp \mu^\pm \mu^\pm$ are forbidden in the SM. They can only occur by lepton mixing involving a non-SM particle, e.g. a Majorana neutrino. The presence of any such decays would therefore be an unambiguous signature of BSM physics.

The LHCb collaboration searched for these decays in a data set corresponding to an integrated luminosity of 1.0 fb^{-1} collected in 2011. As with the search for $D^0 \rightarrow \mu^+\mu^-$, a multivariate algorithm is used to distinguish signal from combinatorial background and particle identification requirements are used to ensure the pions and muons are well identified.

Large resonant contributions to the branching fraction can potentially obscure small signals. To mitigate this effect, the data are divided into bins of the dimuon invariant mass, $m(\mu^+\mu^-)$.

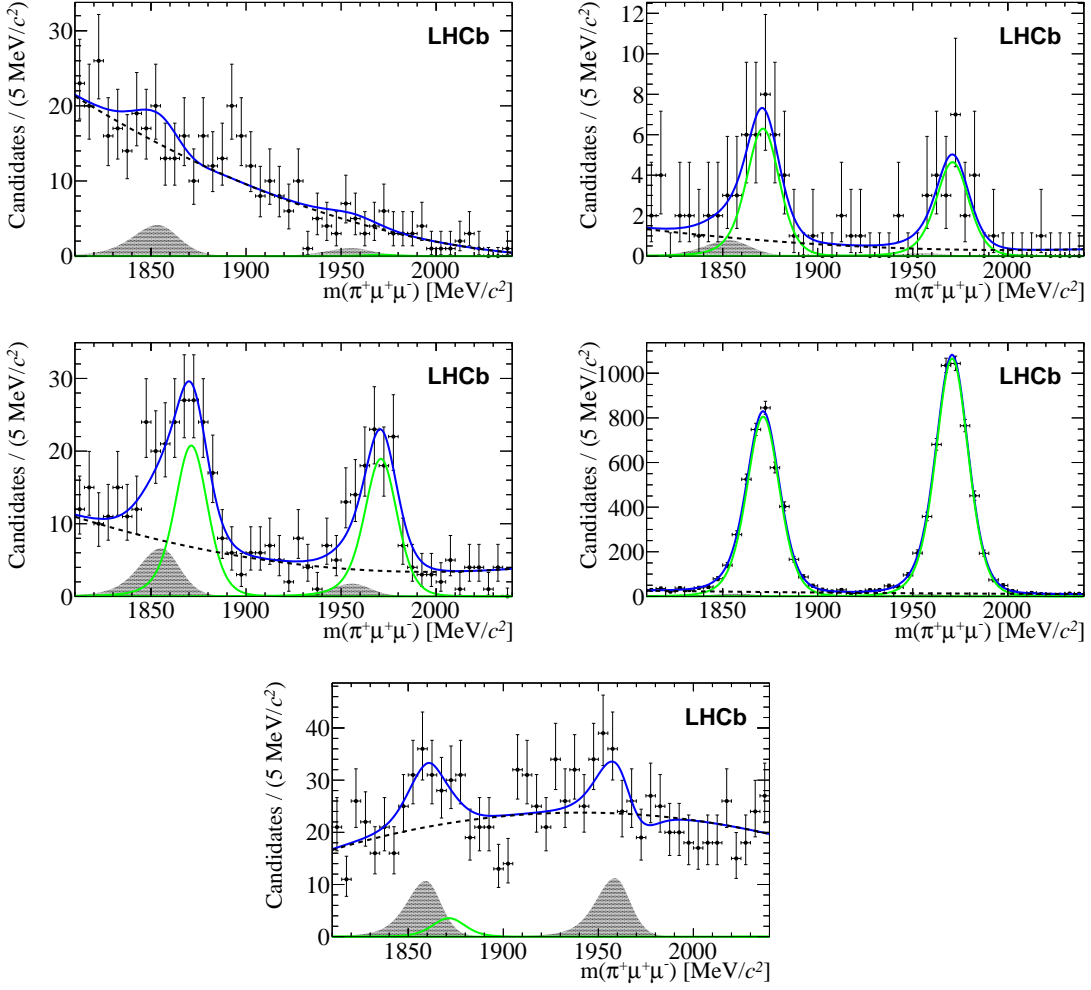


Figure 3: Invariant mass fits to $D_{(s)}^{\pm} \rightarrow \pi^{\pm} \mu^+ \mu^-$ candidates in bins of $m(\mu^+ \mu^-)$. The bins shown are (top left) low- $m(\mu^+ \mu^-)$, (top right) η , (centre left) ρ/ω , (centre right) ϕ , (bottom) high- $m(\mu^+ \mu^-)$. The total PDF is shown as a solid blue line, the signal component is a solid green line, the peaking background is shown as solid grey and the combinatorial background is shown as a dashed black line.

These bins are denoted ‘low- $m(\mu^+ \mu^-)$ ’ (250–525 MeV/ c^2), ‘ η ’ (525–565 MeV/ c^2), ‘ ρ/ω ’ (565–850 MeV/ c^2), ‘ ϕ ’ (850–1250 MeV/ c^2) and ‘high- $m(\mu^+ \mu^-)$ ’ (1250–2000 MeV/ c^2). The abundant resonant decay $D^{\pm} \rightarrow \pi^{\pm} \phi(\mu^+ \mu^-)$, reconstructed in the ϕ bin, is used as normalisation channel. A significant source of background in each bin is the decay $D_{(s)}^{\pm} \rightarrow \pi^{\mp} \pi^+ \pi^-$. Independent mass fits are performed to determine the shape of this component.

A binned maximum likelihood fit to the $D_{(s)}^{\pm}$ mass spectrum is performed in each $m(\mu^+ \mu^-)$ bin, sharing some parameters between bins. Fig. 3 shows the fit in each bin. Clear resonant signals are observed in the η , ρ/ω and ϕ bins, but there is no significant non-resonant signal in the low- and high- $m(\mu^+ \mu^-)$ bins in which decays of interest may lie.

To improve the significance of any BSM signal, reconstructed $D_{(s)}^{\pm} \rightarrow \pi^{\mp} \mu^{\pm} \mu^{\pm}$ candidates are divided into bins of $m(\mu^{\pm} \pi^{\mp})$, assuming such a signal will only appear in one bin. The data are divided into four bins of $m(\mu^{\pm} \pi^{\mp})$: 250–1140 MeV/ c^2 , 1140–1340 MeV/ c^2 , 1340–1550 MeV/ c^2

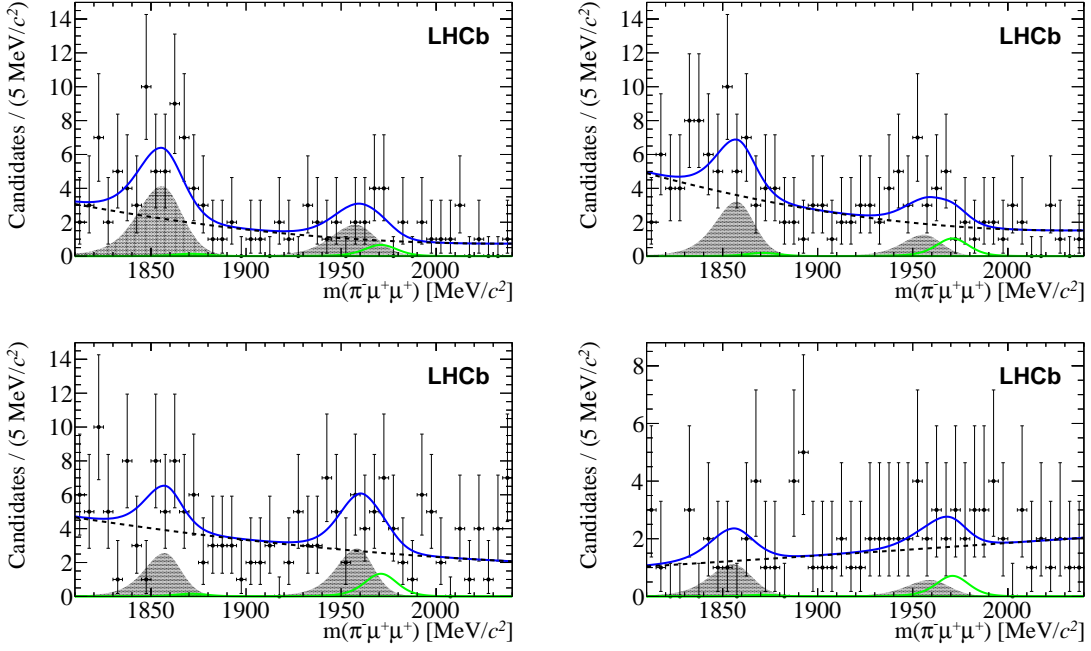


Figure 4: Invariant mass fits to $D_{(s)}^\pm \rightarrow \pi^\mp \mu^\pm \mu^\pm$ candidates in bins of $m(\mu^\pm \pi^\mp)$. The bins shown are (top left) 1, (top right) 2, (bottom left) 3 and (bottom right) 4. The total PDF is shown as a solid blue line, the signal component is a solid green line, the peaking background is shown as solid grey and the combinatorial background is shown as a dashed black line.

and 1540–2000 MeV/ c^2 , which are numbered 1–4 from low to high invariant mass. A binned maximum likelihood fit is performed in each kinematic bin, sharing some parameters between bins. The fits are shown in Fig. 4. No excess over the background is observed for these decay modes.

The determination of the branching fraction $\mathcal{B}(D_{(s)}^\pm \rightarrow \pi\mu\mu)$, where $\pi\mu\mu$ represents both charge combinations, is performed using the formula

$$\mathcal{B}(D_{(s)}^\pm \rightarrow \pi\mu\mu) = \frac{N(D_{(s)}^\pm \rightarrow \pi\mu\mu)}{N(D_{(s)}^\pm \rightarrow \phi(\mu^+\mu^-)\pi)} \times \frac{\varepsilon(D_{(s)}^\pm \rightarrow \phi(\mu^+\mu^-)\pi)}{\varepsilon(D_{(s)}^\pm \rightarrow \pi\mu\mu)} \times \mathcal{B}(D_{(s)}^\pm \rightarrow \phi(\mu^+\mu^-)\pi) \quad (3.1)$$

where $N(X)$ and $\varepsilon(X)$ are the yield and selection efficiency of the final state X , respectively. As in the search for $D^0 \rightarrow \mu^+\mu^-$, efficiencies are taken from Monte Carlo simulated data corrected by data-driven methods, and $\mathcal{B}(D_{(s)}^\pm \rightarrow \phi(\mu^+\mu^-)\pi)$ is taken from Ref. [5].

The CL_s method is used to determine the upper limit on the branching fraction of each decay. The results at 95% C.L., excluding the resonant regions, are

$$\mathcal{B}(D^\pm \rightarrow \pi^\pm \mu^+ \mu^-) < 8.3 \times 10^{-8}, \quad (3.2)$$

$$\mathcal{B}(D_s^\pm \rightarrow \pi^\pm \mu^+ \mu^-) < 4.8 \times 10^{-7}, \quad (3.3)$$

$$\mathcal{B}(D^\pm \rightarrow \pi^\mp \mu^\pm \mu^\pm) < 2.5 \times 10^{-8}, \quad (3.4)$$

$$\mathcal{B}(D_s^\pm \rightarrow \pi^\mp \mu^\pm \mu^\pm) < 1.4 \times 10^{-7}. \quad (3.5)$$

The previous best upper limits for the D^\pm decays to both charge combinations are $\mathcal{O}(10^{-6})$ [12, 13].

4. Conclusions

Searches for rare charm decays are a promising way to reveal the presence of any BSM physics. In these proceedings we have presented two analyses of data collected in 2011 by the LHCb experiment. The first is a search for $D^0 \rightarrow \mu^+\mu^-$ decays and the second is a search for $D_{(s)}^\pm \rightarrow \pi^\pm\mu^+\mu^-$ and $D_{(s)}^\pm \rightarrow \pi^\mp\mu^\pm\mu^\pm$ decays. Upper limits on the branching fractions are set for each final state. These limits represent improvements by a factor of $O(10-100)$ over the previous best measurements, but there are not yet enough data to reach SM-level sensitivity.

An update to the search for $D^0 \rightarrow \mu^+\mu^-$ can be found in Ref. [14]. Both analyses will be extended to use the data set collected by LHCb in 2012.

References

- [1] G. Burdman and I. Shipsey, D^0 - \bar{D}^0 mixing and rare charm decays, *Ann.Rev.Nucl.Part.Sci.* **53** (2003) 431–499, [[arXiv:hep-ph/0310076](#)].
- [2] G. Burdman, E. Golowich, J. L. Hewett, and S. Pakvasa, *Rare charm decays in the standard model and beyond*, *Phys.Rev.* **D66** (2002) 014009, [[arXiv:hep-ph/0112235](#)].
- [3] LHCb collaboration, *Search for the $D^0 \rightarrow \mu^+\mu^-$ decay with 0.9 fb⁻¹ at LHCb*, *LHCb-CONF-2012-005* (2012).
- [4] LHCb collaboration, R. Aaij et al., *Search for $D_{(s)}^+ \rightarrow \pi^+\mu^+\mu^-$ and $D_{(s)}^+ \rightarrow \pi^-\mu^+\mu^+$ decays*, [arXiv:1304.6365](#).
- [5] Particle Data Group, J. Beringer et al., *Review of particle physics*, *Phys. Rev.* **D86** (2012) 010001.
- [6] A. L. Read, *Presentation of search results: The CL(s) technique*, *J.Phys.* **G28** (2002) 2693–2704.
- [7] T. Junk, *Confidence level computation for combining searches with small statistics*, *Nucl.Instrum.Meth.* **A434** (1999) 435–443, [[arXiv:hep-ex/9902006](#)].
- [8] Belle Collaboration, M. Petric et al., *Search for leptonic decays of D^0 mesons*, *Phys.Rev.* **D81** (2010) 091102, [[arXiv:1003.2345](#)].
- [9] A. Paul, I. I. Bigi, and S. Recksiegel, *On $D \rightarrow X_u l^+ l^-$ within the Standard Model and Frameworks like the Littlest Higgs Model with T Parity*, *Phys.Rev.* **D83** (2011) 114006, [[arXiv:1101.6053](#)].
- [10] S. Fajfer, N. Kosnik, and S. Prelovsek, *Updated constraints on new physics in rare charm decays*, *Phys.Rev.* **D76** (2007) 074010, [[arXiv:0706.1133](#)].
- [11] S. Fajfer, S. Prelovsek, and P. Singer, *Rare charm meson decays $D \rightarrow Pl^+l^-$ and $c \rightarrow ul^+l^-$ in SM and MSSM*, *Phys.Rev.* **D64** (2001) 114009, [[arXiv:hep-ph/0106333](#)].
- [12] D0 Collaboration, V. Abazov et al., *Search for flavor-changing-neutral-current D meson decays*, *Phys.Rev.Lett.* **100** (2008) 101801, [[arXiv:0708.2094](#)].
- [13] BaBar Collaboration, J. Lees et al., *Searches for Rare or Forbidden Semileptonic Charm Decays*, *Phys.Rev.* **D84** (2011) 072006, [[arXiv:1107.4465](#)].
- [14] LHCb collaboration, R. Aaij et al., *Search for the rare decay $D^0 \rightarrow \mu^+\mu^-$* , [arXiv:hep-ex/1305.5059](#).